Journal of Geomine (2025), 3(4), 250-262
DOI: 10.22077/jgm.2026.10848.1069

Evaluating the effect of the number of realizations on ore grade modeling and estimation using sequential Gaussian simulation and sequential indicator simulation

Zahra Gholami[1], Hadi Farhadian[1]*, Seyed Amirhossein Adham Hashemi[1]

Received: 2026 Jan. 04, Revised: 2026 May 08, Accepted: 2026 Jun 28, Published: 2026 Jul. 18

ABSTRACT

Geostatistical simulation techniques, including Sequential Gaussian Simulation (SGS) and Sequential Indicator Simulation (SIS), are widely used for ore grade modeling and for assessing spatial uncertainty. However, determining an appropriate number of realizations to achieve stable and reliable results remains a practical challenge in applying these methods. This study investigates the impact of the number of realizations on ore grade modeling results obtained using SGS and SIS. In this research, simulations were performed with different numbers of realizations, including 2, 5, 10, 20, 30, 40, and 50. E-type estimates were then extracted after back-transformation to the original data space. To evaluate the performance of the two methods, the mean bias, coefficient of variation (CV), and percentile-based indices (P10, P50, and P90) were analyzed as functions of the number of realizations. In addition, the results of Sequential Indicator Simulation were compared with those of Sequential Gaussian Simulation. The results indicate that SGS exhibits negligible and stable mean bias across all numbers of realizations and is therefore globally unbiased with respect to the mean. In contrast, SIS when using E-type averaging, shows a significant systematic bias relative to the original data. Moreover, uncertainty measures derived from SGS, including the coefficient of variation and the percentile range, decrease as the number of realizations increases and stablize beyond approximately 20 realizations. Based on these findings, 20 realizations are recommended as an optimal choice, providing an appropriate balance between the stability of uncertainty measures and computational cost. Finally, the three-dimensional E-type model and grade–tonnage curves corresponding to the selected number of realizations are presented, confirming the effectiveness of the proposed approach.

KEYWORDS

Geostatistical simulation; Sequential Gaussian Simulation (SGS); Sequential Indicator Simulation (SIS); number of realizations; ore grade modeling; spatial uncertainty; E-type estimation

I. INTRODUCTION

Modeling the spatial distribution of grade in mineral deposits is invariably associated with significant uncertainty, arising from the inherent heterogeneity of the geological environment and the limitations of exploration data. Classical geostatistical estimation methods, such as kriging, although providing unbiased estimates with minimum variance, compute only a single mean value for each block and are unable to represent the range of variability and the intrinsic uncertainty of the system (Journel and Huijbregts, 1978; Isaaks and Srivastava, 1989; Kaheni et al., 2025). Consequently, the application of geostatistical simulation methods as complementary tools in exploration studies and mineral resource evaluation has received considerable attention.

Geostatistical simulation, by generating a set of equiprobable realizations, enables the representation of different spatial distributions that are all consistent with the original data, the variogram model, and global statistics (Journel, 1994; Shadman and Farhadian, 2023). This characteristic makes simulation a suitable tool for uncertainty analysis, risk assessment, and decision-making at various stages of mine planning (Goovaerts, 1997). Among these methods, Sequential Gaussian Simulation (SGS), owing to its simplicity of implementation and its ability to reproduce the spatial structure of the data, is one of the most widely used

[1] Department of Mining Engineering, Faculty of Engineering, University of Birjand, Birjand, Iran
H. Farhadian: farhadian@birjand.ac.ir

simulation techniques for ore grade modeling (Deutsch and Journel, 1992).

However, SGS is based on the assumption of data normality and requires transformation of the original data into a normal space followed by a back-transformation process. This procedure may lead to errors in reproducing the true data distribution, particularly for highly skewed or multimodal datasets (Emery and Ortiz, 2007). To overcome these limitations, Sequential Indicator Simulation (SIS) was developed. This method does not rely on the normality assumption and operates directly on indicator variables defined by grade thresholds (Journel, 1983).

Indicator simulation is particularly suitable for modeling discontinuous variables, non-normally distributed data, and deposits characterized by sharp grade variations, and it allows for a better reproduction of the original data histogram (Goovaerts, 1994). Nevertheless, this method is also highly sensitive to the choice of the number of realizations, indicator thresholds, and spatial structure. Increasing the number of realizations may alter the statistical behavior of the simulation results (Deutsch et al., 2002).

One important yet relatively understudied issue in geostatistical simulation is the effect of the number of realizations on output statistical indices such as bias, coefficient of variation, and overall uncertainty. A systematic investigation of this effect, especially through a comparison between Sequential Gaussian Simulation and Sequential Indicator Simulation, can provide clearer insights into the selection of an optimal number of realizations for ore grade modeling (Chiles and Delfiner, 2012).

In recent decades, the application of geostatistical methods in Earth sciences, particularly in mining engineering, has significantly increased. These methods, as powerful tools for spatial data analysis, play a key role in reducing uncertainty and improving the accuracy of parameter estimation (Saeid, 2005; Kalantari, 2008; Jalali et al., 2009; Farhadian and Nikvar Hassani, 2020; Aryafar et al., 2020; Farhadian, 2021; Dehshibi et al. 2022; Farhadian and Maleki, 2023; Gonzalez et al., 2025; Saed and Farhadian, 2025; Pangihutan et al., 2026).

Jalali et al. (2009) compared the performance of linear and nonlinear estimators. Their results showed that if the objective is merely point-grade estimation, linear estimators such as kriging perform adequately. However, when the goal is to estimate probability distributions for ore–waste discrimination, even the best linear estimators fail to provide reliable results. In their study, the optimal ore–waste boundary at elevation 2462.5 m in the Sarcheshmeh copper deposit was estimated using indicator kriging and compared with ordinary kriging results.

The application of geostatistics in mineral resource estimation dates back to the introduction of kriging in 1984. Goovaerts demonstrated that indicator kriging, through the use of multiple thresholds, enables non-parametric modeling of uncertain variables and facilitates automated variogram fitting and computational efficiency due to its simplicity (Goovaerts, 2009). Sharifi et al. (2010) emphasized the role of three-dimensional mineral deposit modeling in economic geology studies and reserve estimation. By integrating field observations, exploration boreholes, and drilling data used to determine thickness, they constructed a 3D model of the ore body and estimated proven and probable reserves. Hekmatnejad and Hasani Pak (2011) investigated the estimation of copper grade distribution using nonlinear discrete kriging in the Sungun porphyry copper deposit. Using a custom implementation of discrete kriging, they modeled copper grade distribution and compared the results with ordinary kriging estimates. Yousefi et al. (2011) developed a decision-support algorithm for optimizing exploration operations based on 3D gold deposit modeling. Their approach ranked exploration targets using outputs from the three-dimensional geological model. Daya (2012) estimated the central anomaly reserve of the northern Choghart iron mine using ordinary kriging. Their results confirmed that grade data followed a statistical population, and a spherical variogram model provided the best fit to the experimental variogram. Amini et al. (2015) estimated the reserve of the Lakhshak antimony deposit in Sistan and Baluchestan using Datamine software. Based on statistical analysis and 3D modeling, they reported a total reserve of approximately 77,000 tons with an average grade of 39%. Al-Hassan et al. (2015) compared multiple-indicator kriging and ordinary kriging for the Asuda deposit and reported superior performance of indicator kriging in reserve estimation. Choudhury (2015) compared linear and nonlinear estimators for an iron ore deposit, concluding that indicator kriging provided higher estimation accuracy than ordinary kriging. Yazdani et al. (2016) reviewed geostatistical methods for ore modeling, boundary definition, and reserve estimation. They highlighted the unbiased nature of geostatistical approaches compared to classical deterministic methods and recommended ordinary kriging and indicator kriging for different applications, including ore–waste discrimination and alteration zoning. Ahmadi (2019) evaluated the grade and reserve of the Chah-Bashi iron deposit using block log-kriging, indicator kriging, sequential Gaussian simulation, and inverse distance weighting (IDW). Their results indicated that sequential Gaussian simulation and kriging-based methods provided lower estimation variance compared to IDW. Ahmadi (2020) applied linear and nonlinear geostatistical methods to the Narbaghi copper deposit using SGeMS and Datamine software, comparing log-kriging, multiple indicator kriging, and ordinary kriging results. Mousavi et al. (2021) compared geostatistical methods and artificial neural networks for iron ore grade estimation in central Iran. Their results showed that sequential Gaussian simulation better captured variability compared to kriging, while neural networks provided high predictive accuracy without requiring variogram modeling. Amadu et al. (2022) compared ordinary kriging and inverse distance weighting for the Teberebie paleo-placer gold deposit in Ghana using 19,353 one-meter composites from 706 boreholes. Their results indicated that IDW can produce comparable estimates to kriging under similar conditions. Soleimanzadeh (2022) estimated the reserve of the Shadan gold deposit using IDW and ordinary kriging. Their results showed higher tonnage estimates from kriging compared to IDW, consistent with the findings of the present study.

Accordingly, the main objective of this study is to evaluate the impact of the number of realizations on the results of Sequential Gaussian Simulation and Sequential Indicator Simulation in modeling gold ore grades, and to compare the performance of these two methods in terms of bias, coefficient of variation, and uncertainty. The findings of this research can contribute to a better understanding of the statistical behavior of simulation methods and to more informed selection of simulation parameters in mineral resource evaluation studies.

II. Geostatistical Simulation Method

Geostatistical simulation was first introduced by Journel in the 1970s and has since been widely applied in various fields such as mining, environmental studies, and the oil and gas industry. Geostatistical simulation is a technique for generating data that are consistent with a regionalized variable. A key characteristic of simulated data is their ability to reproduce the statistical properties and spatial variability of the real data (Saeid, 2005, Farhadian and Dehshibi, 2025).

In general, geostatistical simulation provides more effective tools for modeling uncertainty compared to kriging. Over the past four decades, this approach has been extensively used in the estimation, modeling, and evaluation of mineral resources. In each realization, the variable is estimated throughout the deposit in such a way that both the histogram distribution and the variogram of the original data are reproduced (Goovaerts, 1997).

A. Sequential Gaussian Simulation

In geostatistics, the most common simulation method for generating stochastic realizations is Sequential Gaussian Simulation (SGS). Although this method can be implemented exactly, it is generally classified as an approximate technique (Chiles and Delfiner, 2012). In this algorithm, a random simulation path is first defined. Then, using the available conditioning data, kriging is performed at the first location or block, and the mean and variance of the variable at that location are computed using the conditional cumulative distribution function (ccdf). Finally, the simulated value is obtained by sampling from an inverse-normal distribution (Armstrong, 1998).

$$Z_i^{sim} = \widetilde{Z}_\iota + \widetilde{\sigma}_\iota\sqrt{-2(Ln(1-A))}\,cos(2B) \tag{1}$$

In Equation (1), Z_i^{sim} represents the simulated value at the target location. The variables (A) and (B) are random numbers uniformly distributed in the interval (0, 0.99). ($\widetilde{Z}_\iota$) denotes the estimated mean value, and ($\widetilde{\sigma}_\iota$) is the estimated standard deviation at the target location. The simulated value obtained through this process is added to the estimated value at that location (Hengl, 2009).

If this algorithm is applied without conditioning on the original data (i.e., the variable Z_i at locations X_i, i=1,…,n, is simulated without using the original data), the simulation is referred to as unconditional. Conversely, if the simulated values at the data locations are exactly equal to the observed values, the simulation is termed conditional. The basic steps of the Sequential Gaussian Simulation (SGS) algorithm are illustrated in Fig. 1 (Saeid, 2005; Queiroz et al., 2001).

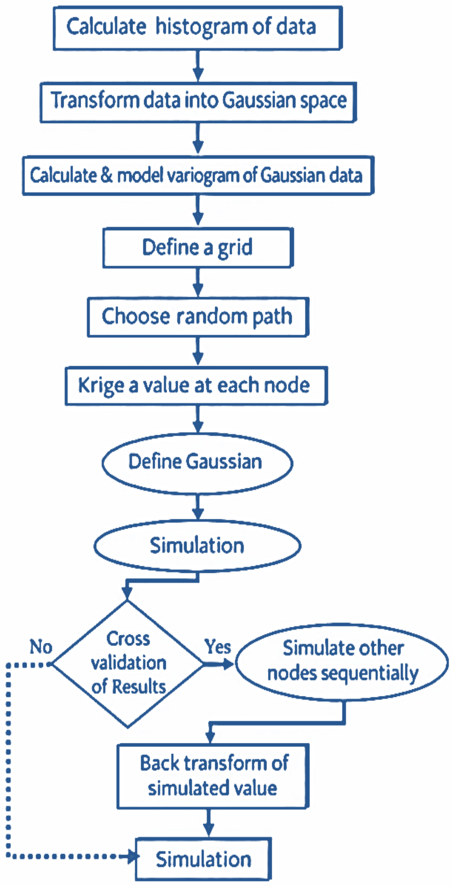

Fig. 1. The basic steps in the SGS algorithm (Saeid, 2005; Queiroz et al, 2001)

B. *Sequential Indicator Simulation*

Sequential Indicator Simulation (SIS) was developed as an alternative to methods that assume data normality and is particularly suitable for non-normally distributed variables, discontinuous data, and deposits characterized by sharp grade variations. SIS is not only used for simulating continuous variables, but it can also simulate discrete variables by applying the fundamental principles of indicator kriging. In this approach, the original variable is transformed into a set of binary (0–1) indicator variables based on a specified cutoff threshold.

$$i(x;z_k) = \begin{cases} 1 & if \quad z(x) \geq z_k \\ 0 & if \quad z(x) < z_k \end{cases} \qquad (2)$$

In Eq. (2), $z(x)$ denotes a continuous grade value at location (x), and z_k represents the cutoff threshold. This transformation is a nonlinear mapping of the original data values into binary codes of 0 and 1 (Goovaerts, 1994). For each threshold, an indicator variogram is computed, and the simulation procedure is carried out like Gaussian simulation, but based on binary variables. The main advantage of this method is that it does not require normal-score transformation and allows for a more accurate reproduction of the empirical data distribution (Goovaerts,1997). The basic steps of the Sequential Indicator Simulation (SIS) algorithm are illustrated in Fig. 2.

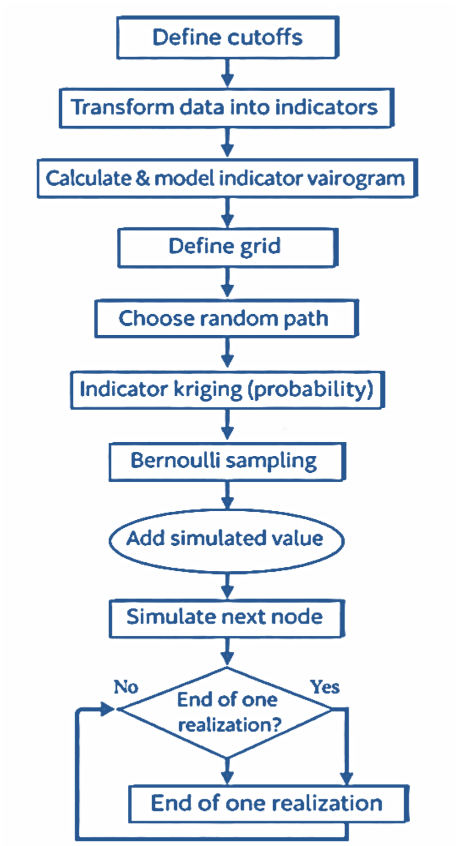

Fig. 2. The basic steps of the SIS algorithm.

III. Simulation Results and Analysis of the Effect of the Number of Realizations

In this study, data from 23 exploration drill holes of the Shadan gold mine, located in South Khorasan Province, approximately 70 km from the city of Khusf, were used. The dataset used in this study consists of three main components: the Assay Table, the Collar Coordinate Table, and the Borehole Survey File. The Assay Table records downhole variations of grade values, including borehole ID, sampling intervals, and assay results. The Collar Table contains spatial coordinates of boreholes (Easting, Northing, elevation) and total drilled depth, while the Survey File defines borehole trajectories through dip and azimuth measurements. The statistical properties of the gold grade data are summarized in Table 1, indicating a strongly positively skewed distribution with high kurtosis, which is characteristic of gold mineralization systems.

After preliminary statistical quality control, the assay data were composited to a uniform length of 1 m, which is consistent with both the average and the most frequent original sample interval, resulting in a total of 6,185 composite samples. For three-dimensional resource modeling, a block model with dimensions of 6 × 6 × 6 m was constructed. This block size was selected after evaluating several candidate dimensions in order to achieve an appropriate balance between local grade selectivity, estimation stability, and computational efficiency.

The studied deposit comprises two distinct mineralized zones, each represented by an independent wireframe corresponding to two spatially separated drillhole clusters (Fig. 3). Following descriptive statistical analysis and assessment of spatial continuity, variography was conducted to characterize the grade continuity structure. The results demonstrated a meaningful spatial correlation, supporting the application of geostatistical methods. The experimental variogram shows a steep increase at the first lag distances, which is consistent with the strong short-range grade variability and nugget effect commonly observed in gold deposits. During model fitting, greater emphasis was placed on the short-distance structure (up to approximately 60 m), as this interval has the strongest influence on the estimation of the selected 6 × 6 × 6 m blocks. Fluctuations observed at larger lag distances were considered less reliable due to the lower number of data pairs. Directional variograms were also examined; however, no clear anisotropy was identified. Therefore, an omnidirectional spherical variogram model was adopted as the most representative model of spatial continuity (Fig. 4).

Geostatistical simulations were carried out using Sequential Gaussian Simulation (SGS) and Sequential Indicator Simulation (SIS) using the Stanford

Geostatistical Modeling Software (SGeMS) for different numbers of realizations, including 2, 5, 10, 20, 30, 40, and 50. In the SGS approach, the data were first transformed into normal-score space, and after generating the realizations, a back-transformation to the original grade space was applied. To enable a direct comparison between the two methods, E-type estimates were calculated from the realizations corresponding to each number of realizations. In the SIS approach, due to the non-normal nature of the data, simulations were performed directly in the indicator variable space, and the corresponding E-type values were extracted.

To assess statistical convergence and the stability of the simulation results, the mean bias, coefficient of variation (CV), and variance uniformity index (UVAR) were computed for each number of realizations and for both methods. The mean bias quantifies the deviation of the results from the original data, CV reflects the relative dispersion of the realizations, and UVAR evaluates the ability of the method to reproduce the data variance.

Table 1. Statistical Properties of Drilling Data

Parameter	Number of Samples	Mean	Standard Deviation	Variance	Skewness	Kurtosis	Minimum	Maximum
Au	6185	0.207	0.268	0.072	4.390	28.953	0.000	2.500

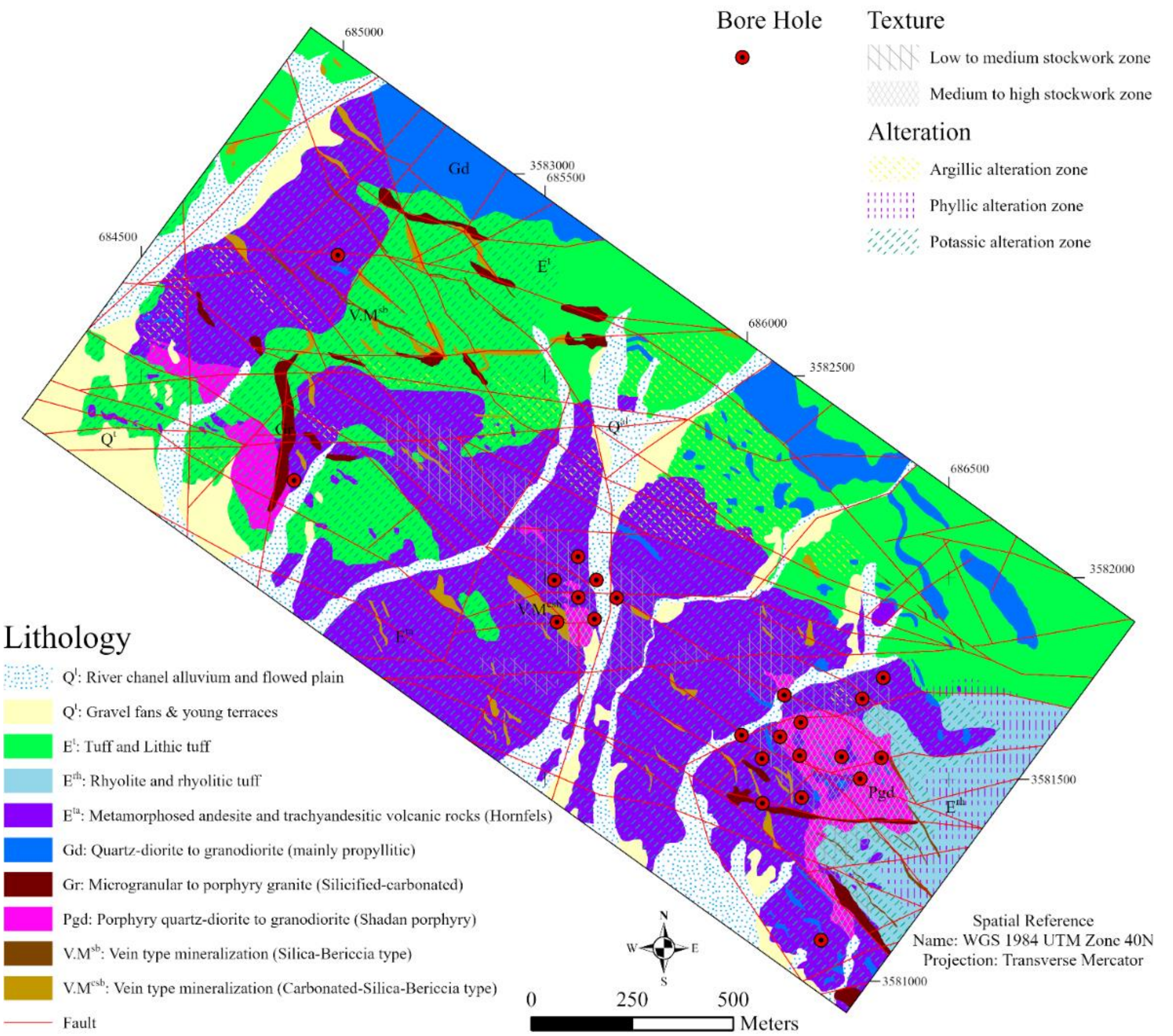

Fig. 3. Display of exploration drill holes in the Shadan gold deposit

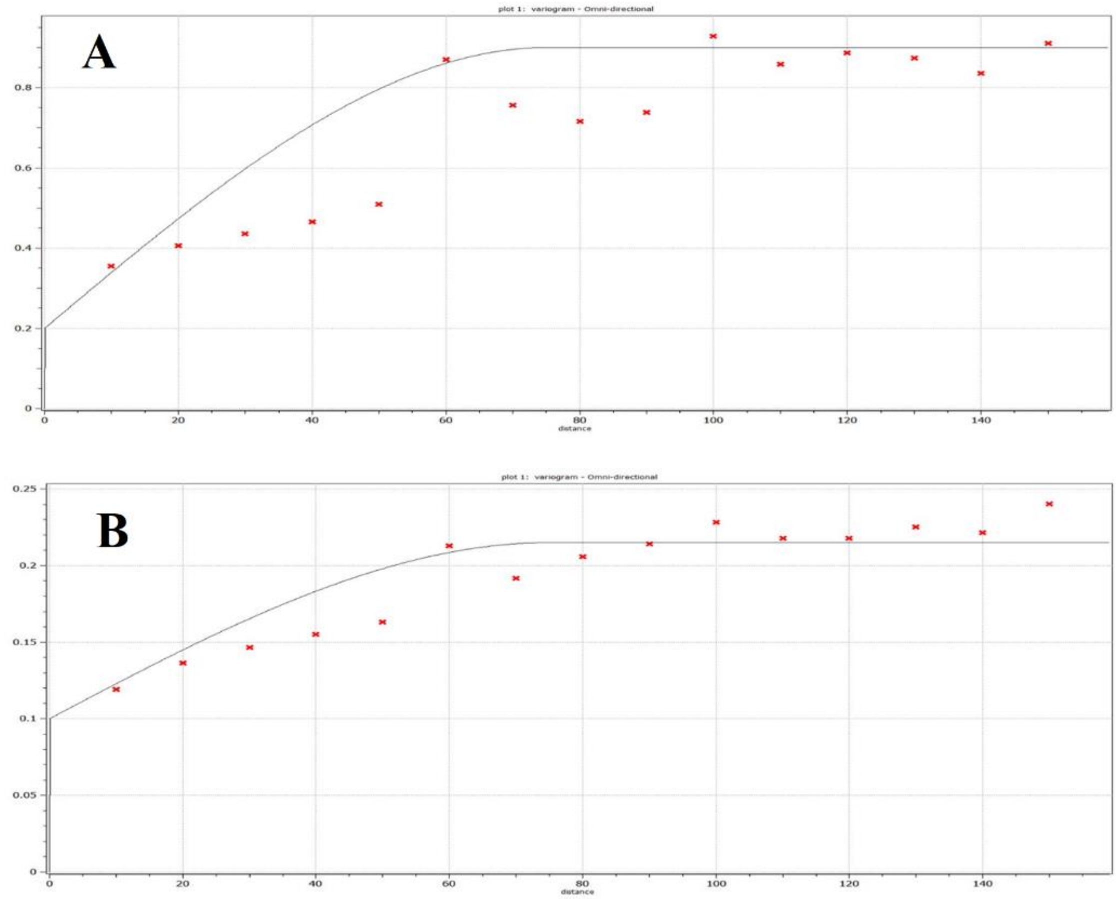

Fig. 4. Omnidirectional variograms of gold grade data used in (A) Sequential Gaussian Simulation and (B) Sequential Indicator Simulation (bottom)

The Mean Bias for K realizations is calculated as the absolute difference between the mean of the simulated results and the mean of the raw data:

$$Bias^{(K)} = | \mu_{sim}^{(K)} - \mu_{raw} | \quad (3)$$

where $\mu_{sim}^{(K)}$ is the mean of the simulated values over K realizations, and μ_{raw} is the mean of the original dataset.

The Coefficient of Variation (CV) of the simulated results is defined as:

$$\mathrm{CV}_{\mathrm{sim}}^{(K)} = \frac{\sigma_{\mathrm{sim}}^{(K)}}{\mu_{\mathrm{sim}}^{(K)}} \quad (4)$$

where $\sigma_{\mathrm{sim}}^{(K)}$ and $\mu_{\mathrm{sim}}^{(K)}$ represent the standard deviation and mean of the simulated values for K realizations, respectively.

To quantify uncertainty, the Uncertainty Variance (UVAR) is calculated as the variance of simulated values across all realizations at each block location:

$$UVAR = \frac{1}{K} \sum_{k=1}^{K} (Z_k - \bar{Z})^2 \quad (5)$$

where Z_k is the simulated value for the kth realization, $\bar{Z}$ is the mean of all realizations at that location, and K is the total number of realizations. UVAR reflects the spatial uncertainty associated with the estimation and provides a quantitative measure of local variability across realizations.

In addition, the uncertainty quantiles $P_{10}^{(K)}$, $P_{50}^{(K)}$, and $P_{90}^{(K)}$ are obtained by sorting the simulated results from the K realizations and identifying the values below which 10%, 50%, and 90% of the data fall, respectively.

As shown in Fig. 5, Sequential Gaussian Simulation exhibits a negligible and nearly constant mean bias of approximately 0.01 across all numbers of realizations, indicating rapid convergence toward the original data statistics after back-transformation. In contrast, Sequential Indicator Simulation displays a larger bias, which increases from approximately 0.14 to 0.17 with an increasing number of realizations, highlighting the greater sensitivity of this method to the number of realizations and to the discrete nature of indicator variables.

The analyses of the coefficient of variation and the variance uniformity index (Fig.s 6 and 7) further demonstrate that, with an increasing number of realizations, Sequential Gaussian Simulation attains a more stable and homogeneous behavior. Conversely, Sequential Indicator Simulation shows greater fluctuations and a slower convergence trend.

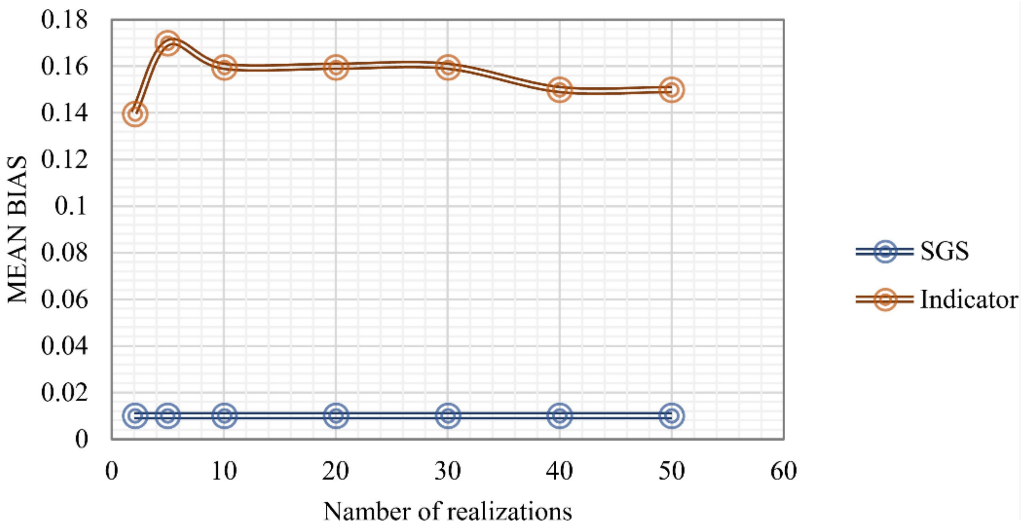

Fig. 5. Variation of E-type mean bias versus number of realizations for SGS and SIS

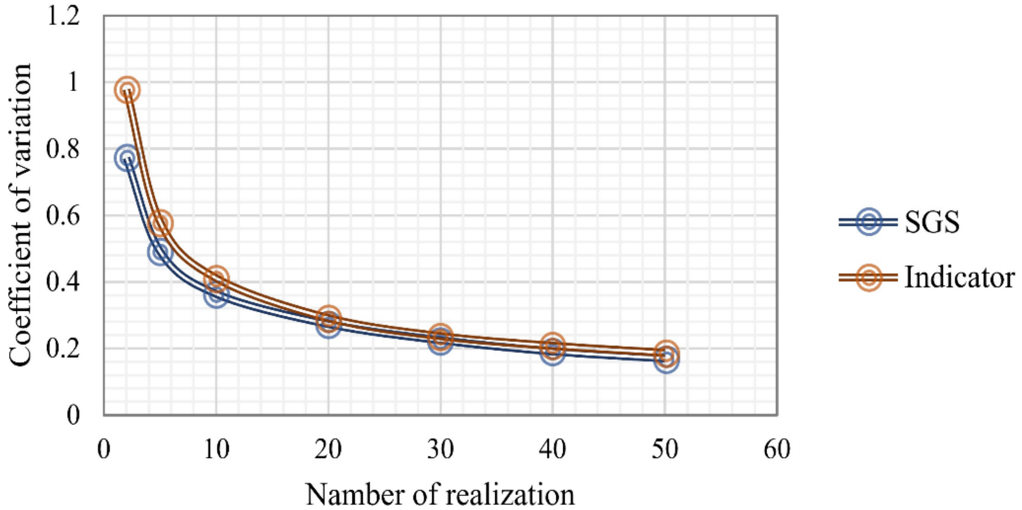

Fig. 6. Coefficient of variation (CV) of the E-type model versus number of realizations for SGS and SIS

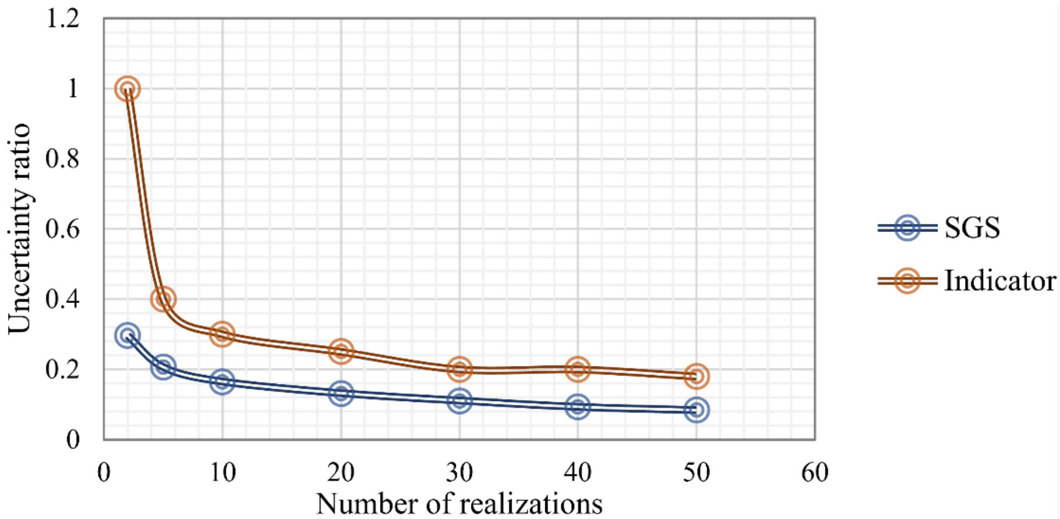

Fig. 7. Variation of E-type uncertainty variance with respect to the number of realizations for SGS and SIS

To investigate the behavior of statistical percentiles and the degree of convergence of simulation results with respect to the number of realizations, the P10, P50, and P90 percentile curves were plotted for both Sequential Gaussian Simulation and Sequential Indicator Simulation. These plots allow evaluation of changes in the low-grade, central, and high-grade portions of the simulated distributions. As illustrated in Fig.s 8 and 9, increasing the number of realizations leads to a reduction in the spacing between percentiles, and the P10, P50, and P90 values reach a relatively stable state beyond approximately n = 20 realizations. Nevertheless, the width of the uncertainty envelope remains larger for Sequential Indicator Simulation than for Sequential Gaussian Simulation, indicating higher uncertainty and greater statistical fluctuations associated with the discrete nature of indicator variables.

Analysis of the trends in the statistical indices shows that beyond 20 realizations, no significant or meaningful improvement in the results is observed, and changes in the indices at higher numbers of realizations are negligible. Accordingly, 20 realizations were selected as the optimal number for subsequent analyses and for the presentation of the final results.

To examine the behavior of data distributions at different stages of the simulation process, histograms of the original grade data, the normal-score transformed data, and the E-type values obtained from Sequential Gaussian Simulation and Sequential Indicator Simulation with 20 realizations were compared. As shown in Fig. 10, the histogram of normalized data indicates that the normal transformation process has been successfully performed. The mean of the data after transformation reached 0.01 and their variance reached 0.96, demonstrating the effective transfer of data into Gaussian space. The results further demonstrate that Sequential Gaussian Simulation reproduces the overall behavior of the data distribution well. In contrast, Sequential Indicator Simulation, despite capturing the general distributional trend, exhibits discrepancies attributable to the discrete nature of indicator variables and the indicator coding process.

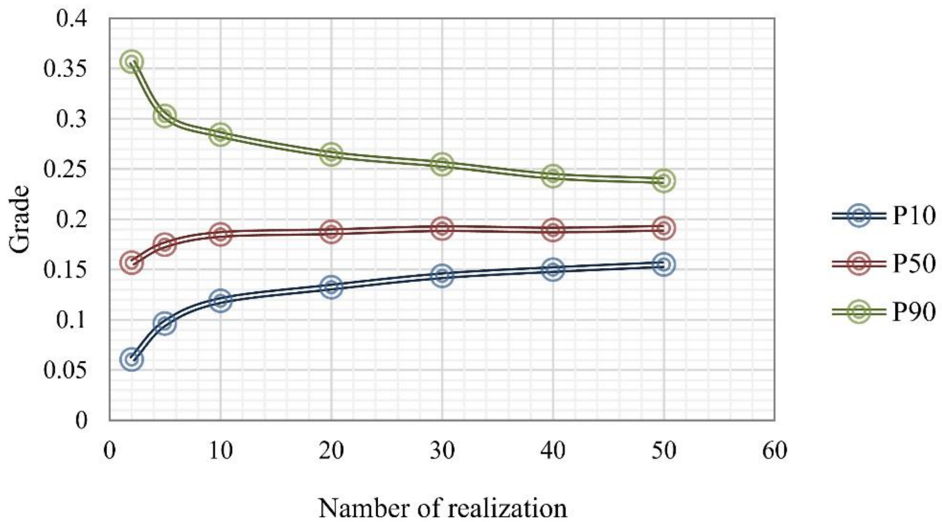

Fig. 8. Trends of P10, P50, and P90 percentiles with increasing number of realizations for the SGS method

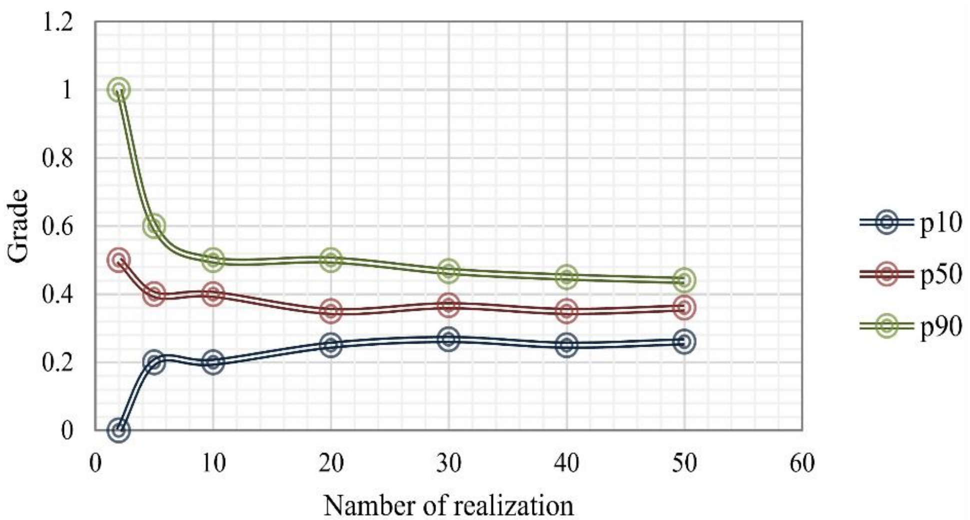

Fig. 9. Trends of P10, P50, and P90 percentiles with increasing number of realizations for the SIS method

Fig. 11 compares the initial data histogram with the E-type histograms obtained from Sequential Gaussian Simulation at different numbers of realizations. In this method, the E-type mean remains constant at 0.19 for all numbers of realizations. As the number of realizations increases, the E-type variance decreases. This is attributed to the nature of the E-type as the mean of multiple realizations, which leads to reduced variance, a smoother distribution, and attenuation of extreme values.

Fig. 12 also shows the E-type histograms obtained from Sequential Indicator Simulation at different numbers of realizations. In the SIS simulation, the E-type variance also decreases with an increasing number of realizations. However, unlike SGS, the E-type mean in SIS is not constant and varies.

To provide a more rigorous comparison between SGS and SIS results, statistical measures were calculated and summarized in Tables 2, 3 and 4, replacing purely visual interpretation of Fig.s 10 and 11. These statistics include minimum, maximum, mean, variance, and median values for both methods under raw and normalized conditions, as well as for different cutoff thresholds.

The results clearly indicate that SGS exhibits lower variance and more stable mean values, reflecting higher statistical stability and faster convergence behavior. In contrast, SIS shows wider value ranges, higher variance, and greater sensitivity to cutoff levels, particularly at higher thresholds where dispersion increases significantly. These characteristics confirm that SIS better preserves local variability and extreme values, but with reduced stability in E-type estimations compared to SGS.

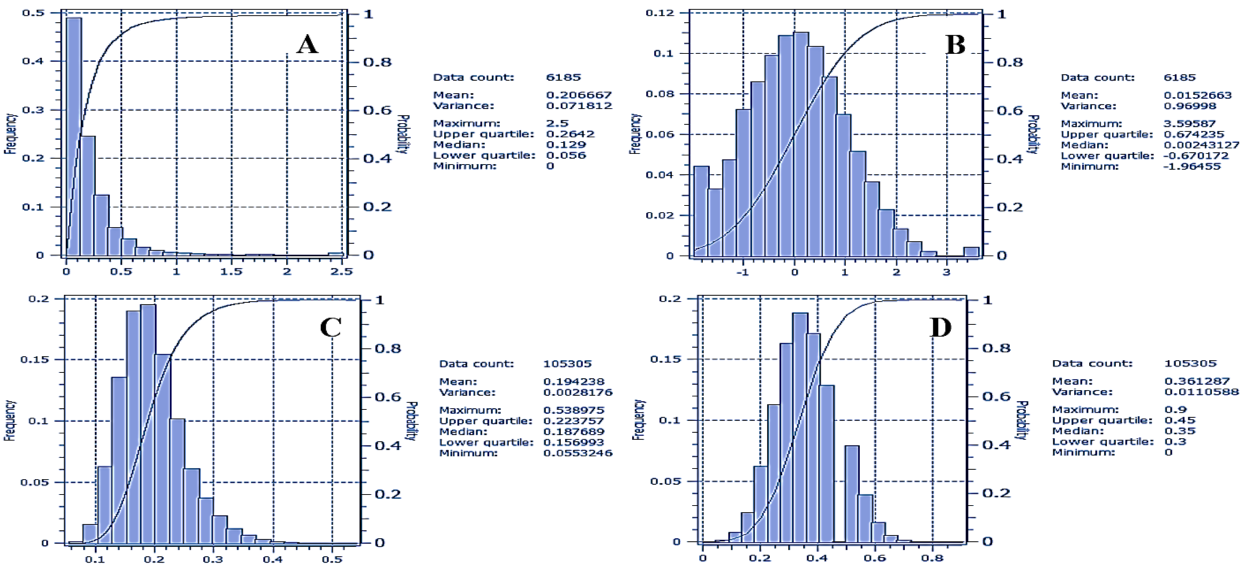

Fig. 10. Comparison of histograms: (A) original data, (B) normal-score transformed data, (C) E-type values obtained from the SGS method, and (D) E-type values obtained from the SIS method for the optimal number of realizations (n = 20).

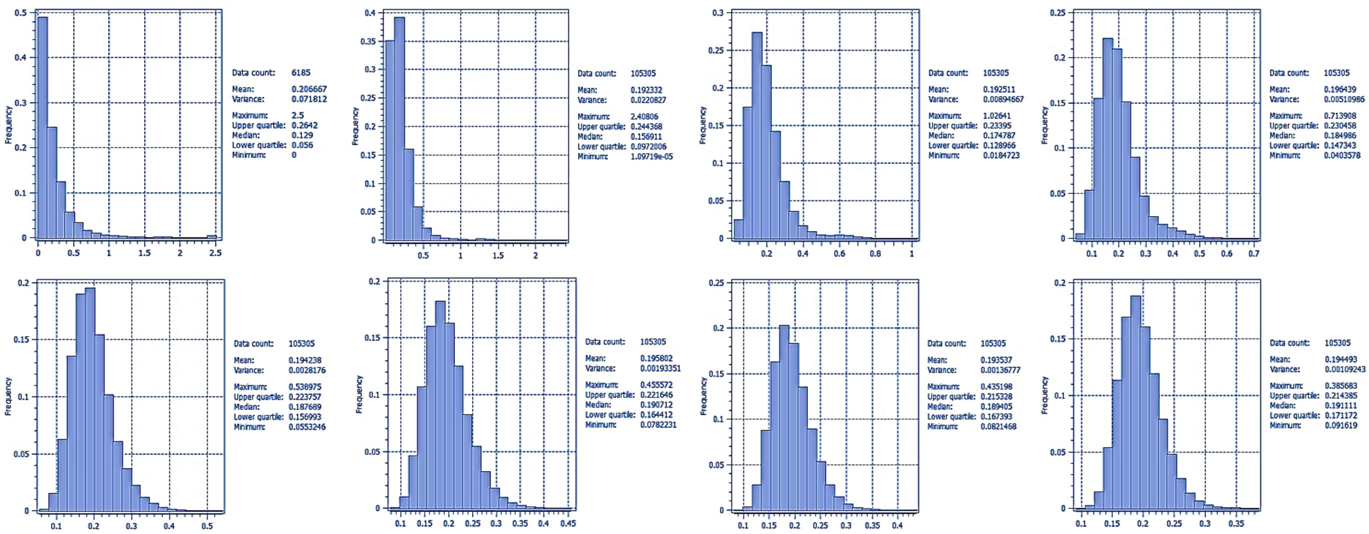

Fig. 11. Histograms of the original data compared with E-type results from the SGS method for different numbers of realizations (2, 5, 10, 20, 30, 40, and 50).

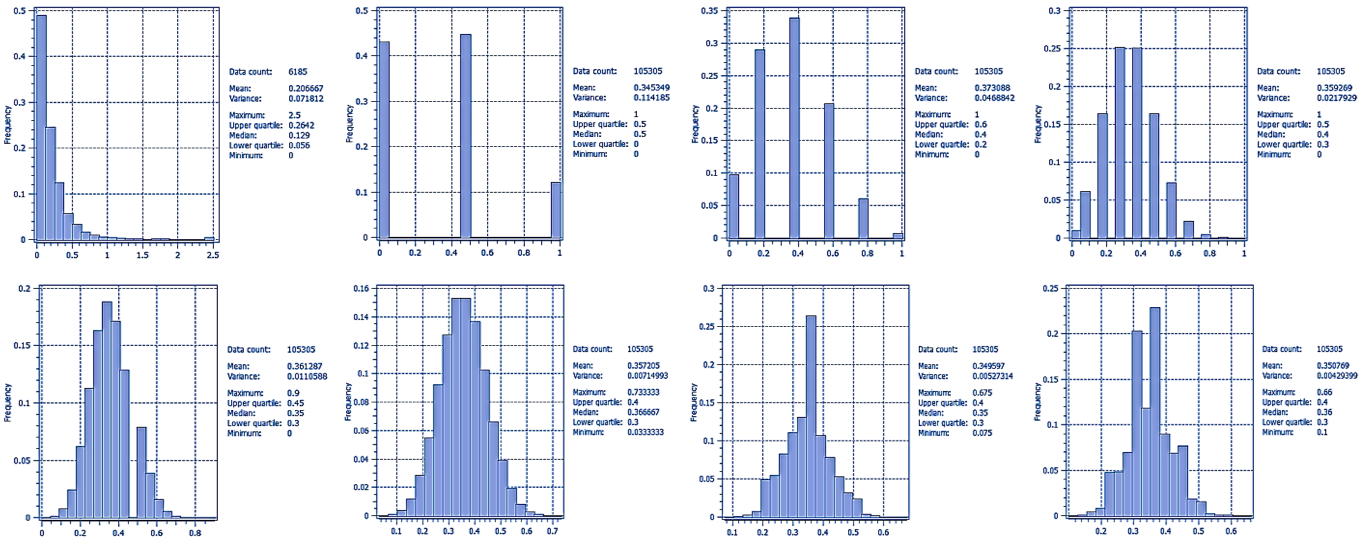

Fig. 12. Histograms of the original data compared with E-type results from the SIS method for different numbers of realizations (2, 5, 10, 20, 30, 40, and 50)

Fig. 12 further evaluates the effect of the number of realizations on SIS E-type results by comparing histograms of the original data with simulated outputs for 2, 5, 10, 20, 30, 40, and 50 realizations. The results show that the distribution progressively stabilizes with increasing realizations, while the most significant improvement occurs up to approximately 20 realizations. Beyond this point, changes in distribution shape and statistical parameters become marginal.

The combined statistical analysis and histogram evaluation confirm that SGS provides more stable and less variable estimates, whereas SIS preserves greater geological variability at the expense of increased uncertainty.

Table 2. Statistical comparison of SGS and SIS results for raw and normalized data, and different realization settings

Parameter	SGS (Raw)	SGS (Normalized)	SIS (Raw)	SIS (Normalized)
Minimum	0.00	0.00	-2.00	0.00
Maximum	0.53	3.5	2.5	9.0
Mean	0.19	0.19	0.20	0.36
Variance	0.003	0.002	0.07	0.015
Median	0.19	0.19	0.07	0.35

Table 3. Statistical measures of SGS and SIS for different cutoff thresholds

Cutoff level	Method	Minimum	Maximum	Mean	Variance	Median
0.09	SGS	0.09	0.53	0.19	0.001	0.19
0.09	SIS	0.10	0.66	0.35	0.004	0.36
0.08	SGS	0.08	0.43	0.19	0.001	0.19
0.08	SIS	0.07	0.67	0.35	0.005	0.35
0.07	SGS	0.07	0.45	0.19	0.001	0.19
0.07	SIS	0.03	0.73	0.35	0.007	0.36
0.05	SGS	0.05	0.53	0.19	0.002	0.19
0.05	SIS	0.00	0.90	0.36	0.010	0.35
0.04	SGS	0.04	0.71	0.19	0.005	0.18
0.04	SIS	0.00	1.00	0.36	0.020	0.40
0.02	SGS	0.02	2.40	0.19	0.020	0.16
0.02	SIS	0.00	1.00	0.34	0.110	0.50
0.01	SGS	0.01	1.02	0.19	0.008	0.17
0.01	SIS	0.00	1.00	0.37	0.040	0.40

Table 4. Summary statistics of original data vs SGS and SIS simulations

Dataset	Minimum	Maximum	Mean	Variance	Median
Original data	0.00	2.50	0.207	0.072	-
SGS	-2.00	0.53	0.190	0.003	0.19
SIS	0.00	3.50	0.360	0.015	0.35

To visualize the spatial distribution of the simulation results and to examine the grade distribution pattern within the deposit volume, three-dimensional ore grade models were generated based on the E-type values obtained from 20 realizations for both simulation methods. These models allow evaluation of spatial continuity, the distribution of high- and low-grade zones, and spatial differences between the two simulation approaches. As shown in Fig. 13, both methods are capable of reproducing the overall deposit pattern; however, Sequential Gaussian Simulation provides a smoother and more continuous grade distribution, whereas Sequential Indicator Simulation exhibits sharper boundaries and greater local variability.

The construction of grade–tonnage curves requires the calculation of corresponding tonnages for different cutoff grades within the deposit. Based on the estimated gold grades, block volumes, and their specific gravities, mineral resources can be calculated for various cutoff grades. According to the grade–tonnage curve shown in Fig. 14, using a cutoff grade of 0.2 ppm Au, the estimated resource tonnage and average gold grade are approximately 24 million tonnes and 0.245 ppm, respectively. Similarly, based on the curve presented in Fig. 15 and using the same cutoff grade of 0.2 ppm Au, the estimated resource tonnage and average gold grade are approximately 58 million tonnes and 0.368 ppm, respectively.

The differences observed in tonnage and average grade between SGS and SIS are mainly related to the inherent characteristics of the two simulation approaches rather than any modeling or computational errors. SGS operates through transformation of the data into Gaussian space followed by back-transformation, which can introduce a smoothing effect and a partial attenuation of extreme values. Consequently, high-grade zones may be slightly reduced, leading to more conservative estimates of both grade and tonnage.

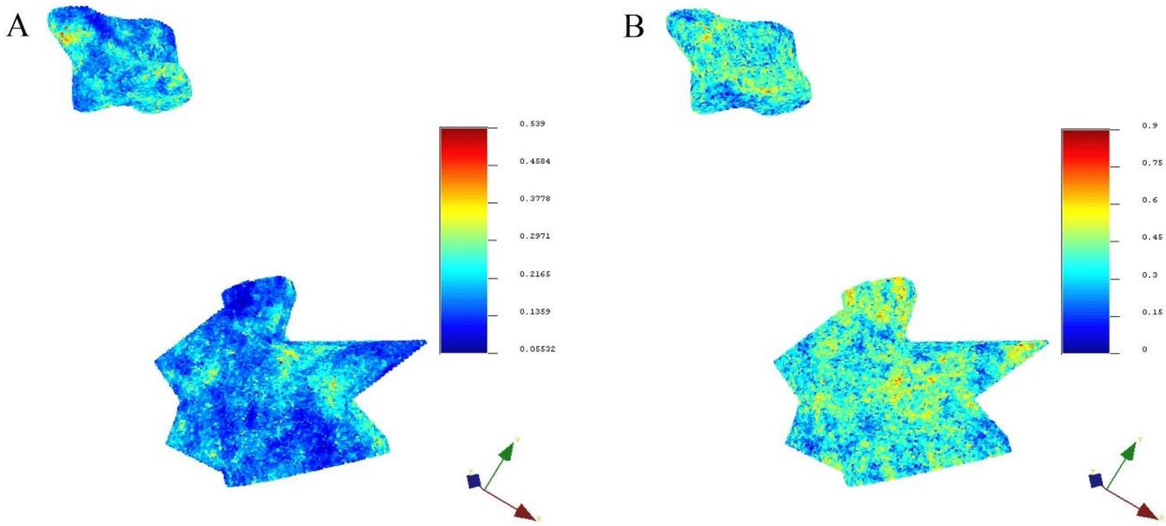

Fig. 13. Block models of ore grade derived from E-type values of Sequential Gaussian Simulation and Sequential Indicator Simulation for n = 20 realizations

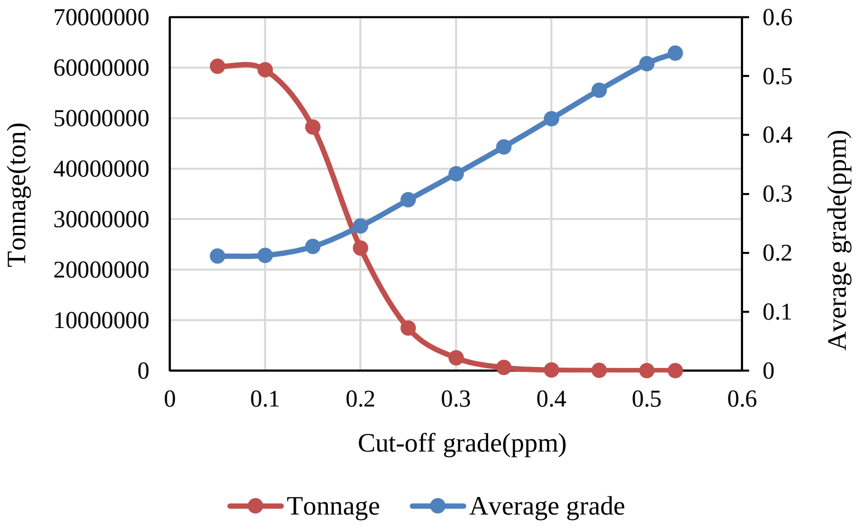

Fig. 14. Grade–tonnage curve derived from Sequential Gaussian Simulation estimates with 20 realizations.

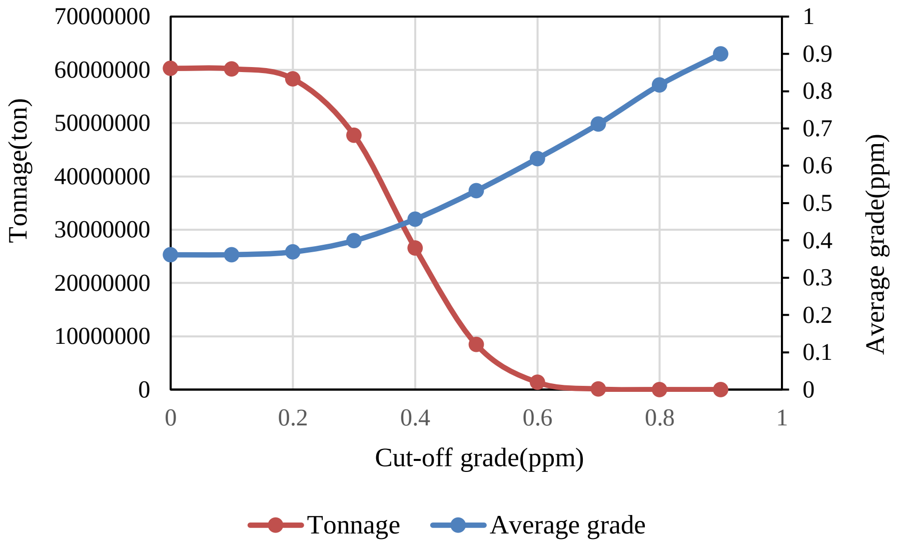

Fig. 15. Grade–tonnage curve derived from Sequential Indicator Simulation estimates with 20 realizations.

In contrast, SIS is based on indicator transformation and threshold modeling, which preserves the local variability and extreme values more explicitly. As a result, SIS tends to reproduce a wider range of grade values and may yield higher tonnage and average grade estimates at the same cutoff levels compared to SGS.

It is also important to note that both methods produce identical results at boundary conditions (i.e., cutoff grade equal to zero and maximum grade), which confirms the correctness and consistency of the implemented modeling workflow. Therefore, the observed discrepancies at intermediate cutoff grades are interpreted as a natural consequence of the different statistical frameworks and underlying assumptions of SGS and SIS, rather than as an indication of error in the simulation process.

IV. Conclusions

This study investigated the influence of the number of realizations on ore grade modeling and uncertainty quantification using Sequential Gaussian Simulation (SGS) and Sequential Indicator Simulation (SIS) for the Shadan gold deposit in eastern Iran.

The results indicate that SGS provides faster statistical convergence and lower estimation bias compared with SIS. The mean bias of SGS remained close to zero across all tested realization numbers, demonstrating its strong capability to reproduce the global statistical characteristics of the original grade data. In contrast, SIS showed relatively higher bias in E-type estimates, mainly due to indicator thresholding, discretization effects, and reconstruction of continuous grades from categorical variables.

Uncertainty measures, including the coefficient of variation (CV), variance uniformity (UVAR), and percentile indicators (P10, P50, and P90), became progressively more stable as the number of realizations increased for both simulation methods. However, the results showed that beyond approximately 20 realizations, further improvements were minor, indicating that additional realizations provide limited practical benefit while increasing computational cost.

The spatial distribution of simulated grades confirmed that both methods successfully reproduced the general mineralization geometry of the deposit. However, SGS generated smoother and more spatially continuous grade patterns, whereas SIS preserved sharper local boundaries and stronger small-scale variability. These differences were also reflected in the grade–tonnage relationships, where SIS generally produced slightly higher tonnage and grade estimates at equivalent cutoff grades.

Overall, the findings demonstrate that increasing the number of realizations beyond an optimal threshold does not necessarily improve modeling performance and may lead to excessive smoothing in E-type models. For the Shadan gold deposit, 20 realizations were identified as an appropriate balance between statistical reliability, uncertainty characterization, and computational efficiency.

From a practical viewpoint, SGS is recommended for mineral resource estimation and mine planning applications requiring unbiased mean estimation and stable uncertainty measures, while SIS may be more suitable when local variability and complex non-Gaussian grade behavior are of primary interest. These results provide a useful guideline for selecting an efficient number of realizations in future geostatistical simulation studies.

References

Ahmadi, R. (2019). Evaluation of grade and reserve of the Chah-Bashi iron deposit using block log kriging, indicator kriging, sequential Gaussian simulation, and inverse distance weighting (IDW). Journal of Advanced Applied Geology, 9(4), 68-82.

Ahmadi, R. (2019). Evaluation of grade and reserve of the Chah-Bashi iron deposit using block log kriging, indicator kriging, sequential Gaussian simulation, and inverse distance weighting (IDW). Journal of Advanced Applied Geology, 9(4), 68-82.

Amini, E., Javaneshir Giv, M., Ariafar, A., and Zeinali, H. (2015). Evaluation of the reserve of the Lakhshak antimony deposit in Sistan and Baluchestan using Datamine software. [Proceedings of the 2nd National Conference on Geology and Exploration of Resources], Shiraz, Iran.

Al-Hassan, S., and Boamah, E. (2015). Comparison of Ordinary Kriging and Multiple Indicator Kriging Estimates of Asuadai Deposit at Adansi Gold Ghana Limited. Ghana Mining Journal, 15(2), 42-49.

Amadu, C. C., Owusu, S., Foli, G., Brako, B. A., and Abanyie, S. A. (2022). Comparison of Ordinary Kriging (OK) and Inverse Distance Weighting (IDW) Methods for the Estimation of a Modified Palaeoplacer Gold Deposit: A Case Study of the Teberebie Gold Deposit, SW Ghana. Earth Science Malaysia, 6(1), 54-63.

Armstrong, M. (1998). Basic linear geostatistics. Springer Science and Business Media.

Aryafar, A., Khosravi, V., and Karami, S. (2020). Groundwater quality assessment of Birjand plain aquifer using kriging estimation and sequential Gaussian simulation methods. Environmental Earth Sciences, 79(10), 210.

Chiles, J. P., and Delfiner, P. (2012). Geostatistics: modeling spatial uncertainty. John Wiley and Sons.

Choudhury, S. (2015). Comparative study on linear and non-linear geo-statistical estimation methods: a case study on iron deposit. Procedia Earth and Planetary Science, 11, 131–139.

Daya, A. A. (2012). Reserve estimation of central part of Choghart north anomaly iron ore deposit through ordinary kriging method. International Journal of Mining Science and Technology, 22(4), 573–577.

Dehshibi, R., Karami, S., Maleki, Z., and Farhadian, H. (2022). A comparative study on evaluation of steady-state groundwater quality in Sirjan's Golgohar mineral zone. Arabian Journal of Geosciences, 15(9), 842.

Deutsch, C. V., and Journel, A. G. (1992). Geostatistical software library and user's guide. New York, 119(147), 578.

Deutsch, C. V., Monteiro, M., Zanon, S., and Leuangthong, O. (2002). Procedures and guidelines for assessing and reporting uncertainty in geostatistical reservoir modeling. Centre for Computational Geostatistics (CCG), 4, 21.

Emery, X., and Ortiz, J. M. (2007). Two Gaussian transform models for change of support problems. Mathematical Geology, 39, 131-154.

Farhadian, H. (2021). A new empirical chart for rockburst analysis in tunnelling: Tunnel rockburst classification (TRC). International Journal of Mining Science and Technology, 31(4), 603–610.

Farhadian, H., and Dehshibi, R. (2025). Geostatistical Analysis of Groundwater Levels at Tangab Dam Using IDW, Kriging, and Sequential Gaussian Simulation. Journal of Hydraulic Structures, 167-187.

Farhadian, H., and Maleki, Z. (2023). Groutability classification of granular soils with cement grouts. Journal of Rock Mechanics and Geotechnical Engineering, 15(6), 1580-1590.

Farhadian, H., and Nikvar-Hassani, A. (2020). Development of a new empirical method for Tunnel Squeezing Classification (TSC). Quarterly Journal of Engineering Geology and Hydrogeology, 53(4), 655-660.

González, J. J., Mery, N., Navarro, F., Díaz, G., Comte, D., and Pichott, S. (2025). Enhancing mining exploration through geostatistical analysis of seismic tomographies at different scales: Improving low-resolution data by high-resolution results. Natural Resources Research, 34(3), 1351–1364.

Goovaerts, P. (1994). Indicator geostatistics for estimating probabilities of exceeding local thresholds. Mathematical Geology, 26, 433-455.

Goovaerts, P. (1997). Geostatistics for natural resources evaluation. Oxford university press.

Goovaerts, P. (2009). AUTO-IK: A 2D indicator kriging program for the automated non-parametric modeling of local uncertainty in earth sciences. Computers and Geosciences, 35(6), 1255–1270.

Hekmatnejad, A., and Hasani Pak, A. A. (2011). Estimation of copper grade distribution using nonlinear discrete kriging: Case study of Sungun porphyry copper deposit. Mining Engineering Journal, 6(12), 1–19.

Hengl, T. (2009). A practical guide to geostatistical mapping (Vol. 52, p. 15). Amsterdam, Netherlands: Hengl.

Isaaks, E. H., and Srivastava, R. M. (1989). Applied geostatistics.

Jalali, M., Rahimipour, G., Riani, M. R., and Taghvaei Nejad, M. (2009). Evaluation of linear and nonlinear kriging estimators in ore–waste block modeling at Sarcheshmeh copper mine. Journal of Earth Sciences, 20(79), 95–100.

Journel, A. G. and Huijbregts, 1978, mining geostatistics. Aca-demic Press, London.

Journel, A. G. (1983). Nonparametric estimation of spatial distributions. Journal of the International Association for Mathematical Geology, 15(3), 445-468.

Journel, A. G. (1994). Modeling uncertainty: some conceptual thoughts. In Geostatistics for the Next Century: An International Forum in Honour of Michel David's Contribution to Geostatistics, Montreal, 1993 (pp. 30-43). Dordrecht: Springer Netherlands.

Kaheni, K., Mokhtari, A. R., and Farhadian, H. (2025). Geostatistical assessment of ore reserve estimation accuracy in the Hired Gold Deposit. Journal of Geomine, 3(3), 155-164.

Kalantari, E. (2008). Geostatistical modeling and reserve estimation of Sungun copper deposit (Master's thesis). Amirkabir University of Technology, Iran.

Mousavi, S., Shayashtafar, M., and Maarefvand, P. (2021). Iron grade modeling using geostatistics and artificial neural networks: Case study of Lakeseah mine, Iran. Journal of Basic and Applied Scientific Research, 73, 27–30.

Paulus Pangihutan, P., Nur Heriawan, M., and Widyatmoko Parnadi, W. (2026, February). Optimization of the Geometrical Model of Quartz Sand in Residual Materials from Alluvial Tin Processing Areas Using a Geostatistical Co-Simulation Method Based on the Drilling and Geophysical Data. In IOP Conference Series: Earth and Environmental Science (Vol. 1590, No. 1, p. 012024). IOP Publishing.

Queiroz, J. C. B., Sturaro, J. R., and Riedel, P. S. (2001, September). Geostatistic Mapping of Arsenic, Manganese and Iron Contamination Risk in the Port of Santana, Amapa, Brazil. In Annual Conf. of Int. Association for Mathematical Geology. Cancun, Mexico.

Saed, S., and Farhadian, H. (2025). A survey on spatial variations of groundwater quality in Kabul, Afghanistan and its evaluation for different uses. Journal of Irrigation Sciences and Engineering, 47(4), 17-34.

Saeid, S. (2005). Deposit estimation and risk estimation by sequential Gaussian geostatistical simulation method. In Proceedings of the Iranian Mining Engineering Conference (pp. 141–154).

Shademan, M., and Farhadian, H. (2023). Contribution of geostatistical modeling on simulating a geomechanical parameter (case study: GSI in Gol-Gohar open pit iron mine, Kerman, southeastern Iran). Journal of Geomine, 1(2), 81-91.

Sharifi, M., and Nourbakhsh, A. (2010). 3D modeling of mineral deposits using exploration data: A case study of Cheshmeh Zangi copper deposit. In 1st International Applied Geological Congress (pp. 1054–1059). Mashhad, Iran.

Soleimanzadeh, M. (2022). Modeling and reserve estimation of Shadan gold deposit using Surpac software (Master's thesis). University of Birjand, Iran.

Yazdani, M., and Alinia, F. (2016). Estimation of copper grade distribution using geostatistics: A case study of Dareh Zareh deposit. 4th International Congress of Civil Engineering, Tehran, Iran.

Yousefi, M., Gholami, R., Kamkarr-Ruhani, A., and Moradzade, A. (2011). Designing of exploration algorithm to generate optimum mineral potential models and management of exploration operation. Geosciences Scientific Quarterly Journal, 21(81), 135–142.